Electronic Supplementary Material (ESI) for Physical Chemistry Chemical Physics.

Supporting Information

Immobilization of Arrestin-3 on different biosensor platforms for evaluating GPCR binding

Saziye Yorulmaz Avsar[*a], Larisa E. Kapinos[*b], Cora-Ann Schoenenberger[a], Gebhard F.X. Schertler [c,d], Jonas Mühle[c], Benoit Meger[c], Roderick Y.H. Lim[b], Martin K. Ostermeier[e], Elena Lesca[c,d**], and Cornelia G. Palivan [a**]

[a] Department of Chemistry and the Swiss Nanoscience Institute, University of Basel, 4002 Basel, Switzerland

[b] Biozentrum and the Swiss Nanoscience Institute, University of Basel, 4056 Basel, Switzerland

[c] Department of Biology and Chemistry, Laboratory of Biomolecular Research, Paul Scherrer Institute, 5303 Villigen-PSI, Switzerland

[d] Department of Biology, ETH Zürich, 8093 Zürich, Switzerland

[e] InterAx Biotech AG, PARK InnovAARE, Villigen, 5234, Switzerland and Paul Scherrer Institute, 5303 Villigen-PSI, Switzerland

*Equal contribution

**Corresponding authors e-mails: cornelia.palivan@unibas.ch and Elena.Lesca@psi.ch

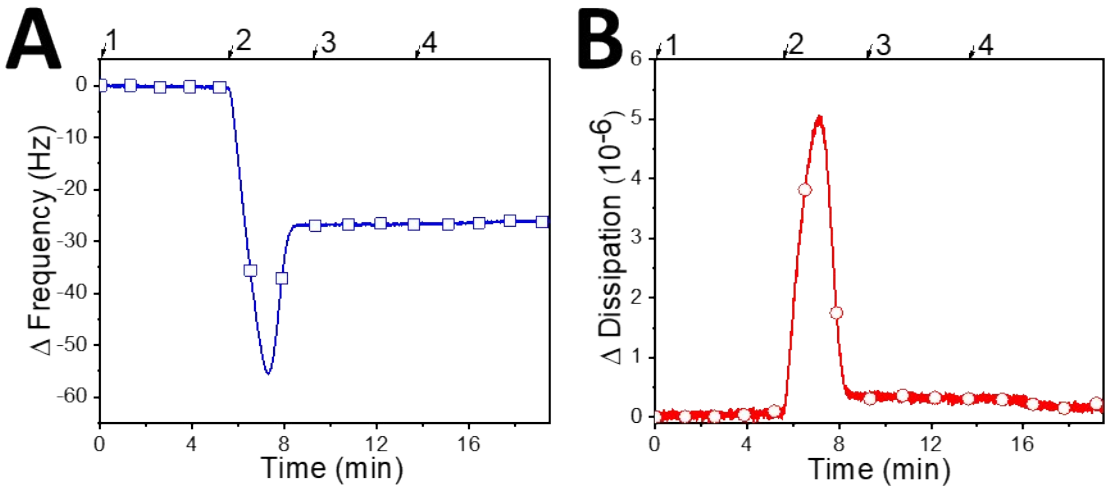

Figure S1. Changes in frequency (**A**) and in dissipation (**B**) were recorded as function of time upon formation of supported lipid bilayers on QCM-D sensors via vesicle fusion. The numbers at the top denote the injection of (1) buffer (20 mM HEPES, 150 mM NaCl at pH 7.4) containing 5 mM $MgCl_2$, (2) vesicles made of POPC:DGS-NTA (Ni^{2+}) (95:5), (3) buffer, and (4) buffer without $MgCl_2$.

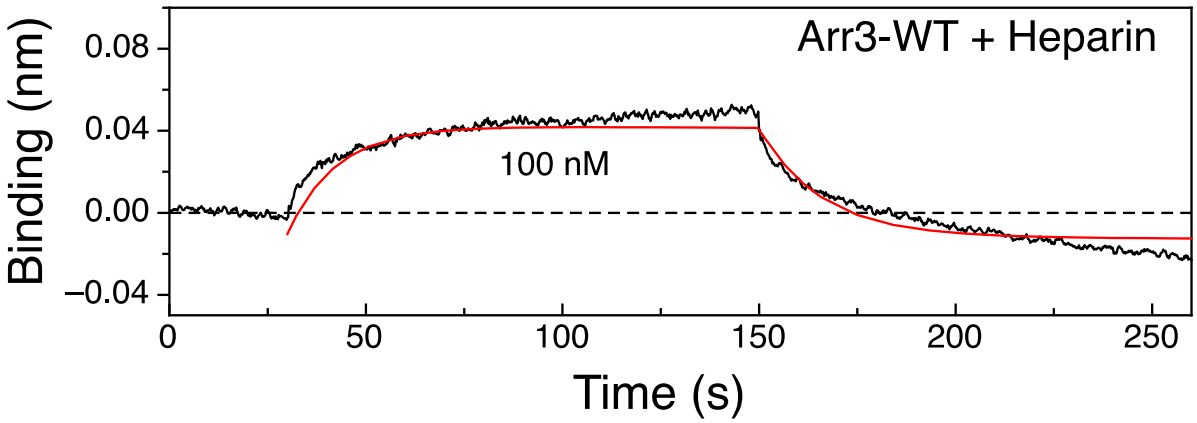

Figure S2. Detection of heparin binding to Arr3-WT on the BLI sensors. Representative heparin (100 nM) binding curve measured by BLI for (A) binding to Arr3-WT immobilized on the Ni^{2+}-NTA tips. Number of replicates, n= 3 for each Arr3-WT.

Table S1. Heparin (100 nM) binding to Arr3-WT

Proteins	K_D, **nM**	$k_a \times 10^5$, $M^{-1}s^{-1}$	k_d, s^{-1}	**Model for kinetic fit**
Arr3-WT	400 ± 3	1.6 ± 0.4	0.064 ± 0.002	1:1 binding

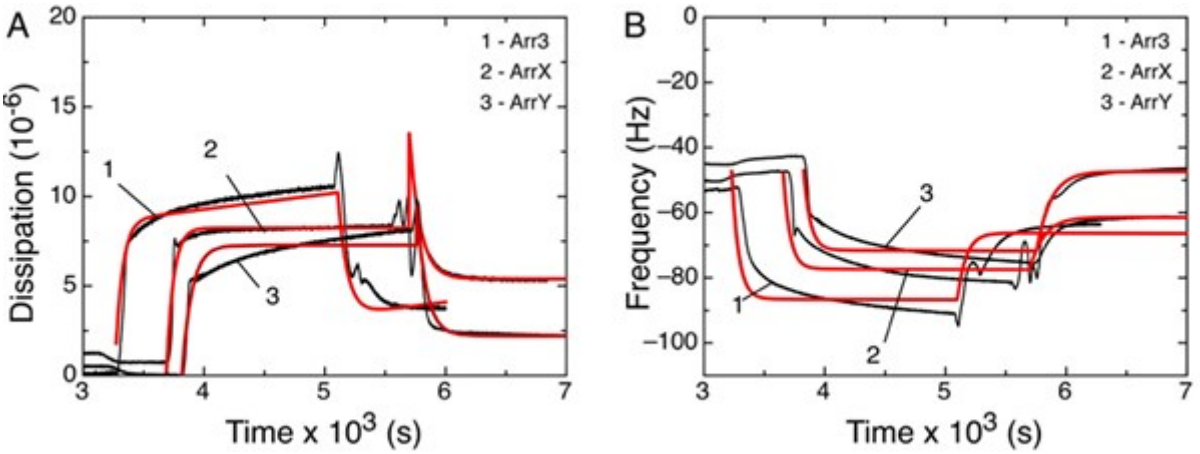

Figure S3. The change in dissipation (A) and frequency (B) in the QCM-D measurements caused by the JSR1 (in DDM micelles) complex formation with arrestin-3 was fitted to the 1:1 binding model. Injected comcentration of JSR1 was 1.59 µM. Measurement was repeated 3 times for each arrestin (n = 3). Obtained kinetic and equilibrium accosiation and dissociation constants are summarized in **Table 6**.

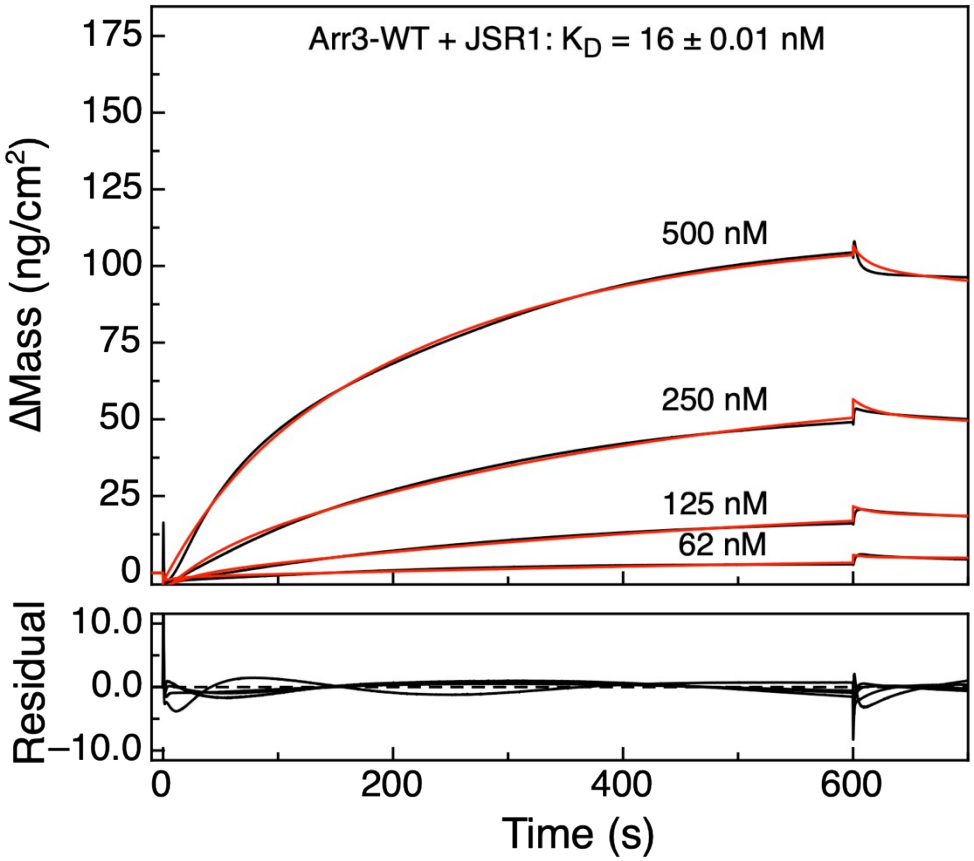

Figure S4. Analysis of JSR1 binding to Arr3-SLM. (A) Representative kinetic fit to 'two-state' model for JSR1 binding to Arr3-WT immobilized on the Ni^{2+}-NTA SLM of HPA sensor chip. Black curves are the experimental data whereas red curves are the fitted data.

Table S2. The equilibrium dissociation constants (K_D) and kinetic association (k_{a1} and k_{a2}) and dissociation (k_{d1} *and* k_{d2}) constants obtained for JSR1 (activated) complexes with Arr3 using SPR. Constants were determined by the data fit to the 'two-state' model. They represent averages ± standard deviations of three independent measurements.

Proteins	K_D, nM*	$k_{a1} \times 10^5$, $M^{-1}s^{-1}$	$k_{a2} \times 10^{-3}$, s^{-1}	k_{d1}, s^{-1}	k_{d2}, $\times 10^{-3}$ s^{-1}	Model for kinetic fit
Arr3-WT	137 ± 6.62	8980 ± 1200	7.86 ± 0.09	306 ± 53	5.29 ± 0.92	Two-state model
Arr3-X	18.0 ± 0.15	0.63 ± 0.006	5.94 ± 0.14	0.02 ± 0.002	3.89 ± 0.14	Two-state model
Arr3-Y	66.2 ± 20	38.7 ± 14	7.92 ± 1.01	0.93 ± 0.35	3.01 ± 0.32	Two-state model

* For 'two-state' model apparent equilibrium dissociation constants was calculated as follows:

$$K_{Dapp} = \frac{k_{d1} \cdot k_{d2}}{k_{a1} \cdot (k_{a2} + k_{d2})}.$$